Available online at www.sciencedirect.com

ScienceDirect

Ceramics International 40 (2014) 4903–4908

CERAMICS INTERNATIONAL

www.elsevier.com/locate/ceramint

Synthesis of neodymium doped yttria nanopowders by microwave-assisted glycine combustion method and the powder characteristics

Nengli Wang*, Xiyan Zhang, Zhaohui Bai

School of Materials Science and Engineering, Changchun University of Science and Technology, Changchun 130022, China

Received 15 September 2013; received in revised form 16 October 2013; accepted 17 October 2013
Available online 26 October 2013

Abstract

Trivalent neodymium ion doped yttria (Nd^{3+}:Y_2O_3) nanopowders were synthesized by using a glycine combustion method. The characteristics of the Nd^{3+}:Y_2O_3 nanopowders with different calcination temperatures and Nd^{3+} ion doping concentrations were analyzed to determine the optimum synthesis conditions of the samples. Thermo-gravimetry and differential scanning colorimetry (TG/DSC), XRD and FTIR analysis showed that the novel glycine-gel microwave combustion method can provide an effective reaction to form yttria nanopowders. The peak positions of the emission spectra of Nd^{3+} ion in yttria host did not differ with the neodymium ion concentration or the calcination temperatures, whereas the luminescence intensities were heavily dependent on the ion concentration and calcination temperatures.

Keywords: A. Microwave processing; C. Optical properties; D. Y_2O_3; E. Functional applications

1. Introduction

Yttrium oxide (Y_2O_3) belongs to the group of cubic-type sesquioxides and has been found many potential applications because of its prominent properties of optical transparency from violet to infrared wavelength range, high mechanical, chemical and thermal stability. Transparent yttria ceramics have been widely used as domes for infrared sensors, light and display component, and solid state laser media, etc. [1–6]. Among them, Nd^{3+}:Y_2O_3 transparent ceramics have been a prominent one. Nd^{3+} ion is one of the earliest trivalent rare earth ions used in solid-state laser and has realized stimulated emission in more than 100 laser host materials. Nd^{3+} ion doped solid-state laser hosts with four level systems have low laser power output threshold, high quantum efficiency, and high stimulated emission cross section [7–9]. So, there have been considerable interests in Nd^{3+}:Y_2O_3 ceramics in recent years [10–13].

Weakly agglomerated nanopowders with spherical morphology are essential to the fabrication of transparent ceramics, because nanocrystalline particles exhibit high surface area and can realize low-temperature sintering for achieving fully-dense ceramics. There are several methods reported for the synthesis of ceramic nanopowders, including precipitation, sol–gel, combustion, and laser evaporation processing [14–19]. Among these methods, combustion synthesis is one of the simple and less time-consuming process techniques that are well recognized for preparing various oxide materials. Microwave assisted combustion synthesis is a novel method to produce ceramic nanopowders, and the heating mechanism of which is different from that of conventional combustion method. In the microwave processing, microwave energy is transferred directly to materials through molecular interaction with the electromagnetic field, and the microwave heating is the transformation of electromagnetic energy to thermal energy, rather than heat transfer. Because microwave radiation penetrates and interacts with molecules, the transfer of electromagnetic energy takes place throughout the volume of the reactants, so can realize volumetric heating. Unlike conventional heating process, microwave processing can offer several advantages, such as more rapid and uniform heating of materials, shorter processing time, and finer particle size, etc [20–22]. In this study, Nd^{3+}:Y_2O_3 nanopowders were synthesized by a microwave-assisted glycine combustion technique. The characterization of structure and luminescence properties of the resulting nanopowders has been reported in the following sections.

*Corresponding author. Tel.: +86 431 8558 3016.
E-mail address: wang_nengli@163.com (N. Wang).

0272-8842/$ - see front matter © 2013 Elsevier Ltd and Techna Group S.r.l. All rights reserved.
http://dx.doi.org/10.1016/j.ceramint.2013.10.073

2. Experimental

The microwave-assisted glycine combustion synthesis involves the dissolution of metal nitrate, which acts as an oxidizer and glycine, which acts as a reducer in deionized water, and a heat treatment of the resulting solution in microwave oven. It was calculated that 3.33 mol of glycine was required to prepare 1 mol of yttria with a complete combustion. The equivalence ratio, i.e., the ratio of the oxidizing valency to reducing valency(O/F) was maintained at unity (O/F=1) [17,20]. Y_2O_3 (99.99%), Nd_2O_3 (99.99%) and glycine (NH_2CH_2COOH) were used as the starting materials. The rare earth raw powders were taken according to the molar ratios of $Y_{2-2x}Nd_{2x}O_3$, x=0.01, 0.02, 0.025, 0.03, respectively. The desired amounts of Y_2O_3 and Nd_2O_3 raw powders were dissolved in nitric acid to obtain a metal nitrate mixture, and then the mixture was diluted with deionized water to a concentration of 0.2 mol/L. The calculated amount of glycine was slowly added into the solution while the solution kept stirring until a clear and homogeneous solution was achieved. The mixed solution was continuously stirred for 3 h to ensure a molecular level mixing, and then was transferred to an alumina crucible and subsequently put into a microwave oven to undergo decomposition in the microwave field of 2.45 GHz. The solution reached the point of spontaneous combustion a few minutes later and started to burn. The combustion sustained for about 8 min, and a foamy and porous precursor powder was obtained. The reaction of assumed complete combustion can be written as:

$$6RE(NO_3)_3+10NH_2CH_2COOH \rightarrow 3RE_2O_3+20CO_2+25H_2O+14N_2$$

where RE=Y, Nd. The obtained precursors were collected and crushed, and then calcined at selected temperatures for 4 h in oxygen atmosphere to obtain crystalline neodymium doped yttria powders.

TG/DSC analysis to the microwave combusted precursor was carried out in N_2 atmosphere with the heating rate of 10 °C/min from room temperature to 1200 °C on a NETZSCH-STA409PC thermal analyzer. XRD measurements was conducted on a Rigaku Ultima IV diffractometer with Cu$K\alpha$ radiation source (λ=1.5406 Å) for phase identification, characterization of grain size and lattice parameters of the samples. Fourier transformation infrared spectroscopy (FTIR) of the as-prepared precursor and the calcined powders was measured on a Shimadzu FTIR-8400S spectrometer in the range of 4000–400 cm^{-1} using the standard KBr method. The morphology and particle size distribution of Nd^{3+}:Y_2O_3 nanopowders were studied by a high resolution FEG scanning electron microscope (FE-SEM, Model XL30, FEI Company). The emission spectra of the Nd^{3+}:Y_2O_3 nanopowders were measured using a spectrofluorometer (Model Fluorolog-3, Jobin Yvon Spex) at room temperature.

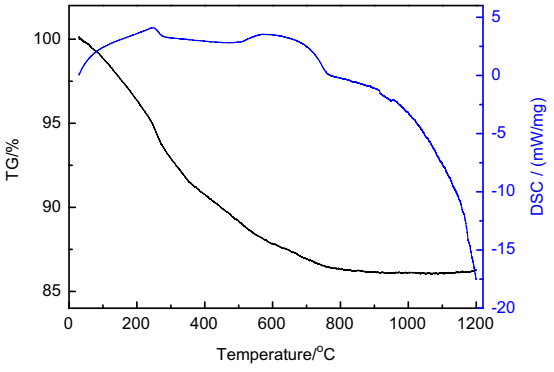

Fig. 1. TG/DSC curves of the Nd^{3+}:Y_2O_3 precursor.

3. Results and discussion

3.1. Thermal analysis

Fig. 1 shows the TG/DSC results of the as-prepared precursors. The TG analysis showed the weight losses of 13.7% for the glycine-combustion precursor. The weight loss is mainly due to the removal of absorbed moisture and excess gaseous products in the as-prepared powders because of the highly absorptive property of nanopowder products [17,20]. The weight of the precursor remained constant when heating temperature was above 800 °C, indicating the decomposition of the precursor completed and no changes in the phase composition.

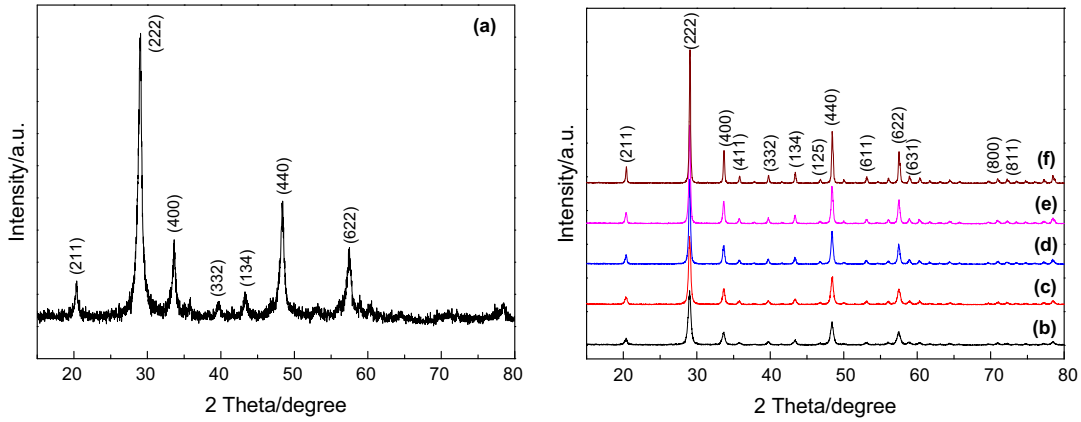

Fig. 2. XRD patterns of (a) as-prepared precursor and powders calcined at (b) 700 °C; (c) 800 °C; (d) 900 °C; (e) 1000 °C and (f) 1100 °C.

3.2. Structure characterization

X-ray diffraction patterns of 1 at% Nd^{3+}:Y_2O_3 precursor and powders calcined at different temperatures are shown in Fig. 2. The precursor displayed a partially crystallization, which showed peaks of (2 1 1), (2 2 2), (4 0 0), (3 3 2), (1 3 4), (4 4 0), and (6 2 2) of yttria phase already. This indicates that the formation of single-phase cubic crystalline yttria nanopowders was facilitated in microwave field itself, and also the high efficiency of the glycine microwave combustion. With the increase of calcination temperature, all of the characteristic XRD peaks of yttria appeared when calcined at 700 °C, and the diffraction peaks agreed well with that of cubic Y_2O_3 crystal structure (JCPDS Card No. 41-1105). The diffraction intensity increased with the increase of calcination temperature, indicating the growth of crystal and a complete crystallization of pure phase cubic yttria during heat treatment. Grain size of the precursor and powders calcined at different temperatures was determined by X-ray line broadening and calculated by using the Scherrer's formula:

$$D = \frac{0.89\lambda}{\sqrt{\beta_{sample}^2 - \beta_{ref}^2}\cos\theta}$$

where D is the grain size diameter (nm), λ is the wavelength of Cu$K\alpha$ radiation source ($\lambda = 1.5406$ Å), β_{sample} is the full-width at half-maximum (FWHM) of a diffraction peak at an angle θ and β_{ref} corresponds to the instrumental FWHM. The calculated grain size is presented in Table 1. It can be seen that the precursor powder is ultra-fine, and the grain size of the powder increases with the increase of calcinations temperature. All the grain sizes are in a nanometer scale.

Fig. 3 shows the X-ray diffraction patterns of Nd^{3+}:Y_2O_3 nanopowders calcined at 1100 °C with different Nd doping concentrations. It can be seen that the patterns match well with

Table 1
Calculated grain size by Scherrer's formula.

Temperature (°C)	Precursor	700	800	900	1000	1100
Size (nm)	17.1	26.8	34.3	51.4	61.2	72.9

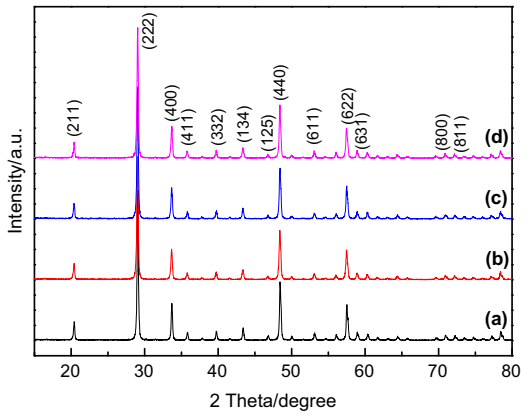

Fig. 3. XRD patterns of Nd^{3+}:Y_2O_3 nanopowders with Nd^{3+} doping concentration of (a) 1 at%; (b) 2 at%; (c) 2.5 at% and (d) 3 at%.

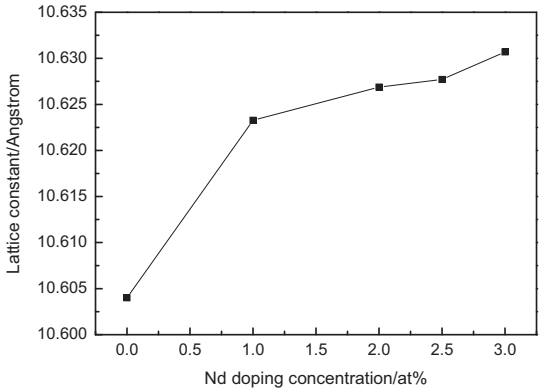

Fig. 4. The dependence of lattice constant from Nd content in Y_2O_3.

JCPDS Card No. 41-1105, indicating the formation of a solid solution of Nd in the cubic yttria. The lattice constants calculated from the XRD patterns are 10.62327, 10. 62688, 10.6277, and 10.63069 Å for 1.0, 2.0, 2.5, and 3.0 at% Nd^{3+}:Y_2O_3, respectively. The lattice parameter values are greater than that of the pure yttria ($a=b=c=10.604$ Å for Y_2O_3, JCPDS No. 41-1105). The dependence of lattice parameter from Nd doping concentration is shown in Fig. 4. The introduction of neodymium ion into yttrium oxide results in a non-linear increase of its lattice constant.

The FTIR method was employed to characterize the structural evolution versus temperature of the powder samples, and the results is shown in Fig. 5. The FTIR curves of the precursor and calcined powders are concise and almost identical. The results show them to be free of organic by-products. The weak absorption bands at 3444 and 1646 cm^{-1} are attributed to O–H stretching and bending vibration respectively, which was caused by the moisture present on the surface of the powders. The weak absorption band at 2355 cm^{-1} in the precursor belongs to unsymmetrical stretching of the residual CO_2, which was produced in the reaction and absorbed on the precursor powder. After calcining above 800 °C, the band disappeared, indicating the removal of CO_2. Absorption bands below 576 cm^{-1} are attributed to the metal–oxide (M–O) vibration, indicating the complete crystallization of Y_2O_3. Also, the absence of secondary peaks in the XRD patterns of calcined powders supports FTIR results. The FTIR spectra obtained are in accordance with the TG/DSC and XRD result.

3.3. FE-SEM analysis

Fig. 6 shows the morphologies of the 1 at% Nd^{3+}:Y_2O_3 precusor and nanopowders calcined at different temperatures. During the microwave-assisted combustion process, the generation of the gaseous products, including N_2, CO_2 and H_2O as water vapour increased the surface area of the precursor by creating micro and nanoporous, so the precursors have low density and a foamy and fluffy appearance (Fig. 6(a)). During calcinations, the precursor began to break into nanometric particles, the particle size increased with the rise of calcination temperatures. There was a rapid increase of particle size

between 800 and 1000 °C, and the powder calcined at 1000 °C has a spherical morphology with a homogeneous particle size of about 80 nm. When calcined at 1100 °C, the morphology of the powder is mainly spherical, and the particle size increased slightly to about 90 nm. Combined with the XRD and FE-SEM analysis, it can be seen that powders prepared by the glycine microwave-assisted combustion techniques have the characteristics of pure phase, homogenous morphology and particle size distribution.

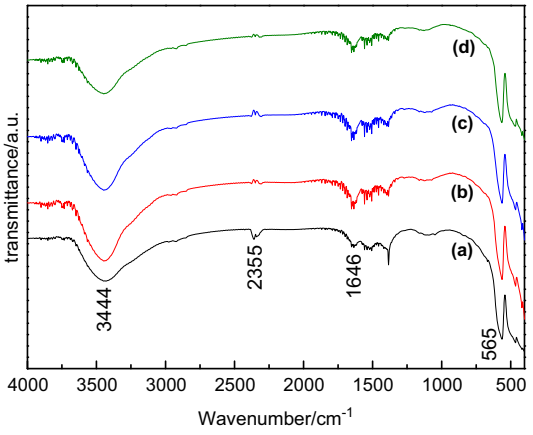

Fig. 5. FTIR spectra of (a) the precursor and powders calcined at (b) 800 °C; (c) 1000 °C; (d) 1100 °C.

3.4. Photoluminescence spectra

Fig.7 shows the emission spectra of Nd^{3+}:Y_2O_3 nanopowders calcined at different temperatures. Emission bands centered at 1078.6 and 1357.1 nm are corresponding to $^4F_{3/2} \rightarrow {}^4I_{11/2}$ and $^4F_{3/2} \rightarrow {}^4I_{13/2}$ transitions of Nd^{3+} ions, respectively [7,23]. The strongest peak is at 1078.6 nm, and this is a wavelength of laser output when the Nd^{3+}:Y_2O_3 transparent ceramics are used as a laser media [7]. It can be seen that with the increase of calcinations temperature, the luminescence intensities of the sample increased, the powder calcined at 1000 °C has the highest luminescence intensity. And then, the luminescence intensity decreased when the powder was calcined at 1100 °C.

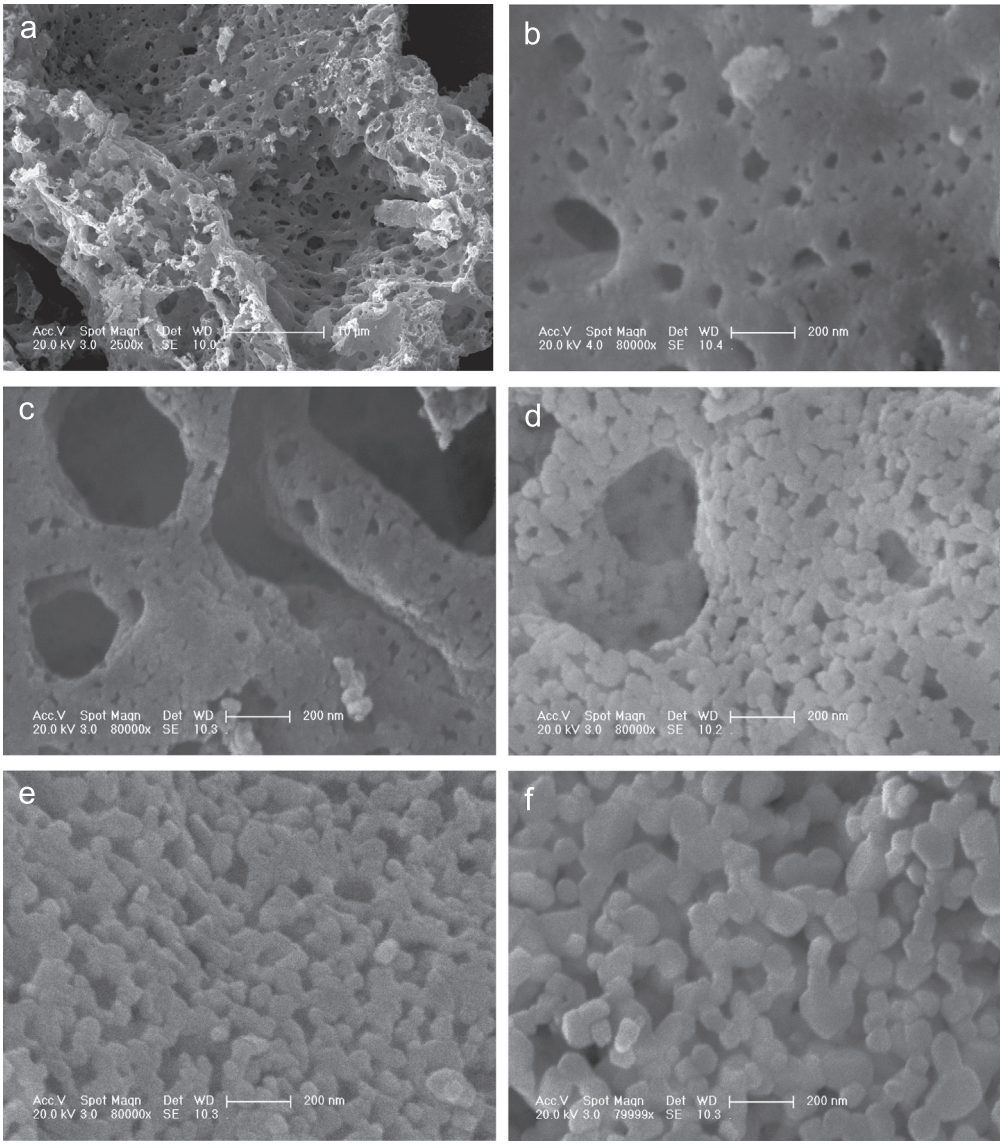

Fig. 6. FE-SEM images of (a) the precursor and powders calcined at (b) 700 °C; (c) 800 °C; (d) 900 °C; (e) 1000 °C and (f) 1100 °C.

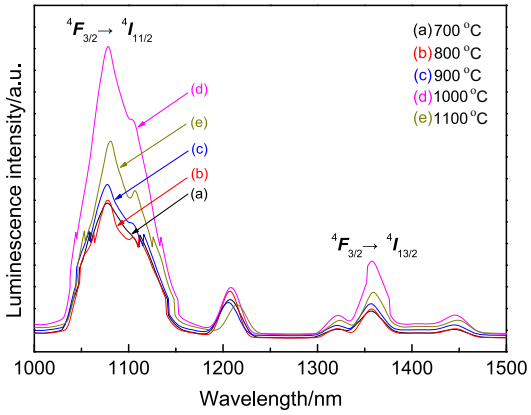

Fig. 7. Emission spectra of Nd^{3+}:Y_2O_3 nanopowders calcined at different temperatures (λ_{ex}=808 nm).

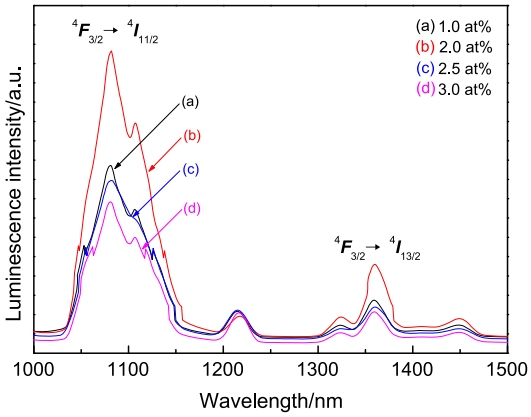

Fig. 8. Emission spectra of Nd^{3+}:Y_2O_3 nanopowders with different Nd^{3+} concentration (λ_{ex}=808 nm).

Fig. 8 shows the emission spectra of the nanopowders with different Nd^{3+} ion content. It can be seen that the greatest luminescence intensity was obtained from the powder sample with Nd^{3+} ion doping concentration of 2 at%, and the luminescence intensity was obviously dependent on the neodymium ion doping concentration. When the Nd^{3+} ion doping concentration was less than 2 at%, the luminescence intensity improved with the increase of the doping concentration value. However, when the value was higher than 2 at%, the luminescence intensity heavily decreased because of the concentration quenching effect of the Nd^{3+} ions.

4. Conclusions

Nd^{3+}:Y_2O_3 nano-sized powders were prepared by a microwave-assisted glycine solution combustion method. The synthesized powders had a cubic-phase crystal structure with homogeneous powder morphology and a narrow particle size distribution. The calcined powder with Nd doping concentration of 2 at% has the highest fluorescence intensity. The strongest peak centers at 1078.6 nm wavelength, which is corresponding to $^4F_{3/2}\rightarrow {}^4I_{11/2}$ transition of Nd^{3+} ions. There were no differences in the emission peak position in the samples with different synthetic conditions, whereas the luminescence intensities of the samples varied with the calcination temperatures and the doping concentrations of Nd^{3+} ions.

Acknowledgements

Financial support from Changchun University of Science and Technology (Contract no. 2008B0678) is gratefully appreciated.

References

[1] T.R Hinklin, S.C. Rand, R.M. Laine, Transparent, polycrystalline upconverting nanoceramics: towards 3-D displays, Adv. Mater. 20 (2008) 1270–1273.
[2] G. Bernard-Granger, C. Guizard, L. San-Miguel, Sintering behavior and optical properties of yttria, J. Am. Ceram. Soc. 90 (9) (2007) 2698–2702.
[3] H. Eilers, Fabrication, optical transmittance, and hardness of IR-transparent ceramics made from nanophase yttria, J. Eur. Ceram. Soc 27 (2007) 4711–4717.
[4] Y.L. Kopylov, V.B. Kravchenko, A.A. Komarov, Z.M. Lebedeva, V.V. Shemet, Nd:Y_2O_3 nanopowders for laser ceramics, Opt. Mater. 29 (2007) 1236–1239.
[5] J. Kong, D.Y. Tang, B. Zhao, J. Lu, K. Ueda, H. Yagi, T. Yanagitani, 9.2-W diode-end-pumped Yb:Y_2O_3 ceramic laser, Appl. Phys. Lett. 86 (2005) 161116.
[6] G.Q. Xie, D.Y. Tang, L.M. Zhao, L.J. Qian, K. Ueda, High-power self-mode-locked Yb:Y_2O_3 ceramic laser, Opt. Lett. 32 (18) (2007) 2741–2743.
[7] G.A. Kumar, J. Lu, A.A. Kaminskii, K.I. Ueda, H. Yagi, T. Yanagitani, Spectroscopic and stimulated emission characteristeics of Nd^{3+} in transparent Y_2O_3 ceramics, IEEE. J. Quantum Electron. 42 (7) (2006) 643–650.
[8] Q.H. Yang, C.G. Dou, J. Ding, X.M. Hu, J. Xu, Spectral characterization of transparent $(Nd_{0.01}Y_{0.94}La_{0.05})_2O_3$ laser ceramics, Appl. Phys. Lett. 91 (2007) 111918.
[9] X. Hou, S. Zhou, T. Jia, H. Lin, H. Teng, Effect of Nd concentration on structural and optical properties of Nd:Y_2O_3 transparent ceramic, J. Lumin. 131 (2011) 1953–1958.
[10] A. Fukabori, M. Sekita, T. Ikegami, N. lyi, T. Komatsu, M. Kawamura, M. Suzuki, Induced emission cross section of a possible laser line in Nd:Y_2O_3 ceramics at 1.095 μm, J. Appl. Phys. 101 (2007) 043112.
[11] A. Fukabori, V. Chani, J. Pejchal, K. Kamada, A. Yoshikawa, T. Ikegami, Fundamental optical constants of Nd-doped Y_2O_3 ceramic and its scintillation characteristics, Opt. Mater. 34 (2011) 452–456.
[12] K. Laishram, R. Mann, N. Malhan, Effect of complexing agents on the powder characteristics and sinterability of neodymium doped yttria nanoparticles, Powder Technol 229 (2012) 148–151.
[13] Z. Huang, W. Guo, Y. Liu, Q. Huang, F. Tang, Y. Cao, Synthesis of Nd:Y_2O_3 nanopowders leading to transparent ceramics, Mater. Chem. Phys. 128 (2011) 44–49.
[14] X. Ji, B. Kang, J. Deng, H. Huang, X. Wang, Thermal decompositon and evolved gas anlysis of neodymium-doped yttrium aluminum garnet precusor prepared by co-precipitation, Thermochim. Acta 552 (2013) 23–27.
[15] Y. Huang, D. Jiang, J. Zhang, Q. Lin, Z. Huang, Synthesis of monodispersed spherical Nd:Y_2O_3 powder for transparent ceramics, Ceram. Int. 37 (2011) 3523–3529.
[16] A. Leleckaite, A. Kareiva, H. Bettentrup, T. Jüstel, H.-Jürgen Meyer, Sol–gel preparation and characterization of codoped yttrium aluminium garnet powders, Z. Anorg. Allg. Chem. 631 (2005) 2987–2993.
[17] R.V. Mangalaraja, J. Mouzon, P. Hedström, I. Kero, K.V.S. Ramam, Carlos.P. Camurri, M. Odén, Combustion synthesisi of Y_2O_3 and Yb-Y_2O_3 Part I. Nanopowders and their characterization, J. Mater. Process. Technol. 208 (2008) 415–422.
[18] Yu.V. Orlovskii, A.V. Popov, V.V. Platonov, S.G. Fedorenko, I. Sildos, V.V. Osipov, Fluctuation kinetics of fluorescence hopping quenching in the Nd^{3+}:Y_2O_3 spherical nanoparticles, J. Lumin. 139 (2013) 91–97.

[19] A.S. Kaygorodov, V.V Ivanov, V.R. Khrustov, Yu.A. Kotov, A.I. Medvedev, V.V. Osipov, M.G. Ivanov, A.N. Orlov, A. M. Murzakaev, Fabrication of Nd:Y_2O_3 transparent ceramcis by pulsed compaction and sintering of weakly agglomerated nanopowders, J. Eur. Ceram. Soc. 27 (2007) 1165–1169.

[20] R.V. Mangalaraja, J. Mouzon, P. Hedström, Carlos.P. Camurri, S. Ananthakumar, M. Odén, Microwave assisted combustion synthesis of nanocrystalline yttria and its powder characteristics, Powder Technol. 191 (2009) 309–314.

[21] A.K. Sharma, R. Krishnamurthy, Microwave processng of sprayed alumina composite for enhanced performance, J. Eur. Ceram. Soc. 22 (2002) 2849–2860.

[22] M. Rekha, K. Laishram, R.K. Gupta, N. Malhan, A.K. Satsangi, Energy-efficient green synthesis of Nd:Y_2O_3 nanopowder by microwave gel combustion, J. Mater. Sci. 44 (2009) 4252–4257.

[23] D.K. Sardar, D.M. Dee, K.L. Nash, R.M. Yow, J.B. Guber, Optical absroption intensity analysis and emission crosss sections for the intermanifold and the inter-Stark transitions of $Nd^{3+}(4f^3)$ in polycrystalline ceramic Y_2O_3, J. Appl. Phys 100 (2006) 123106.